TU DELFT

BACHELOR THESIS

Understanding and predicting ice growth on Dutch lakes and canals

Author:
Daniël HOONHOUT

Supervisor:
Prof.dr.ir. B.J.H. VAN DE WIEL
dr. P. BAAS
J.G. IZETT

A thesis submitted in fulfillment of the requirements for the degree of Bachelor of Science

in the

Faculty of Civil Engineering and Geoscience
Department of Geoscience and Remote Sensing

February 11, 2019

TU DELFT

Abstract

Faculty of Civil Engineering and Geoscience
Department of Geoscience and Remote Sensing

Bachelor of Science

Understanding and predicting ice growth on Dutch lakes and canals

by Daniël HOONHOUT

Ice, present on lakes and canals, can lead to social and economic consequences. For example inland shipping can be hindered due to ice or, more favourable, sport events can be held like ice skating. Predicting ice thickness can therefore be quite useful. Existing ice prediction models are already integrated into meteorological institutes across the world. The goal of this study is to understand the physics of ice growth, and to assess how ice growth is affected by various meteorological factors, like local temperature, radiation and wind velocity. The understanding of the physics behind these meteorological factors can be used to improve existing and future models.

The following meteorological factors and their effects on ice growth are investigated: temperature, atmospheric heat resistance, radiation, precipitation, wind velocity and atmospheric stability. With atmospheric stability we refer to the fact that the temperature stratification has an effect on the effectiveness of heat exchange in the lower atmosphere. The factors are implemented into an ice prediction model, building up complexity. The prediction models are run using idealised weather data (focusing on a single meteorological parameter), giving an insight to the effects of the meteorological factors concerning the ice growth. Also the prediction models are compared to observed ice data applying contemporary weather data in the area around the observations.

It appears to be rather difficult to asses the quality of the prediction, due to the fact that the observed ice data has a relatively large spread. Nevertheless, it can be concluded that the final model's estimates are quite reasonable, as the prediction lays within the bounds of the spread (in all the data sets). The effects of the various meteorological forcing factors are quite clearly visible. To initiate the ice growth the atmospheric temperature needs to be below 0°C, hence the temperature is of vital importance. The effect of atmospheric stability on vertical heat exchange needs to be incorporated into the models to prevent overestimation of the ice growth. When an initial ice layer is present, higher wind velocities causes the ice to grow more rapidly and vice versa. Radiation can influence the ice growth rate both positively and negatively, depending on the cloud coverage and the solar radiation. The radiation (coherent with cloud coverage) also creates an asymmetry between the growing and the melting rate of ice. Snowfall slows down ice growth (melt) rate considerably, due to its isolating properties.

It is recommended to look further into the effects of snowfall, as there possibly could be an asymmetry of its effect on ice growth between the melting and growing stage of ice, due to variations of thermal conductivity and albedo between 'fresh' snow layers and melting snow layers. The stability conditions can not be implemented directly into the model, because determining the stability (at a given time) requires the use of iterative methods, which in turn requires more computational time. It is recommended to further investigate how to simulate these conditions, possibly by varying the roughness lengths (height from the surface where the temperature gradient can be assumed zero) of ice. Altogether, this study offers a good insight into the effects and physics of the investigated meteorological factors (apart from atmospheric stability) to ice growth.

Acknowledgements

I would like to thank all my supervisors for aiding me throughout this project: Bas van de Wiel for getting me excited to investigate this subject, and challenging me with various physical/mathematical problems. Peter Baas for providing me all the necessary data which I needed dearly at every stage of the project. And last, but definitely not least: Jonathan Izett for answering all of my many questions and for being a huge help during the writing process.

Contents

List of Figures

List of Tables

Chapter 1

Introduction

Ice layers entail various consequences, for example inland shipping can be obstructed due to ice. This can lead to unwanted economical consequences in the shipping industry. On a positive note, the ice can bring a lot of recreational activity and sport events, like the ice skating contest, 'de Elfstedentocht', in the Netherlands. A rather large amount of money and endeavour is involved in the realisation of a national event of this magnitude. Last-minute cancelling of the tournament due to insufficiently large ice thicknesses could therefore be disastrous. These are a few of the many reasons why prediction of ice growth is important.

Existing prediction models are already used by official authorities worldwide. For example, the Royal Netherlands Meteorological Institute (KNMI) predicts ice growth on lakes and canals based on a model of De Bruin and Wessel from 1998, henceforth called BW88. The operational KNMI model is a one-layer model in which the entire water column is described by a single value of temperature, predicting the water temperature, ice and snow thickness (De Bruijn, Bosveld, & Van Der Plas, 2014). Another model with comparable predictive power to the operational KNMI model has been supplied by the Leibniz Institute of Freshwater Ecology (FLake). This model is based on the self-similarity of the thermal structure of the water column (De Bruijn et al., 2014).

Apart from the permanent layers of ice at the Earth's poles, the growth of ice in lakes and canals is a recurring seasonal phenomenon across the globe. The growth of ice depends on a large range of meteorological and physical parameters. The challenge in predicting ice growth lies in determining the importance of these parameters, and to construct a mathematical model that is both effective and simple. Simplicity makes it easily accessible and fast computationally.

This study mainly focuses on the effect of several meteorological factors on ice growth, the physical reasons why these factors effect ice growth and how this can be translated into a model. After getting a proper understanding, ice growth is predicted for a few cases to test the validity of this model. We stress that this (short) preliminary study is primarily for interpretation purposes. The goal is not the replace operational models. That being said, understanding the effects of a wide spectrum of meteorological parameters can be useful to improve future models.

This report is built up as follows: In chapter 2 the physical background of various meteorological factors is introduced, with a focus on how these factors influence ice growth. The simple ice growth model is presented in chapter 3, with complexity built up through subsequent inclusion of the various meteorological parameters. In chapter 4 the models are validated using historical weather data, and observed ice thicknesses across the Netherlands. Also, to better understand the effects of the meteorological parameters, the models are assessed for idealised input data, specific, individual parameters varied. The results of the models are analysed in chapter 5, discussing the validity of the models and assumptions. Finally, in chapter 6,

conclusions are made about the effects of the tested parameters on the ice growth. Recommendations are made about how to implement certain parameters into future models.

Chapter 2

Theoretical background

Various physical processes such as convection and radiation have an important role when it comes to ice growth. The theoretical and physical reasons as to *why* and, to some degree, *how* these processes influence the ice growth, are explained in this chapter. The equations describing these phenomena and how they are implemented in the ice model will be discussed in Chapter 3

2.1 Heat transfer

In order for a liquid to solidify, the temperature of the liquid needs to drop below its melting point. The melting point of water is henceforth called the freezing point. To change the phase of water, thermal energy needs to either be added or removed from the water. In order for thermal energy to move, three basic processes take place: conduction, convection and radiation (Haberman, 2014).

2.1.1 Conductive heat transfer

Due to the colliding of neighbouring molecules, kinetic energy of vibration of one molecule is transferred to its nearest neighbour (Haberman, 2014). This process is called conduction. During conductive heat transfer, thermal energy is therefore spread, even though the molecules themselves don't move their location appreciably (Haberman, 2014). Because of the latter, within the (solid) ice layer heat transfer is mainly conductive.

2.1.2 Convective heat transfer

In (Haberman, 2014) it is stated that if an 'air package', with vibrating, moving molecules within it i.e, carrying thermal energy - moves from one region to another (by fluid motion), it takes its thermal energy with it. This type of movement of thermal energy is called convection. When water or air travels in any direction, their thermal energy travels with them. Therefore, phenomena which can cause these currents in the air or water (such as transport by wind) are looked into.

2.1.3 Heat transfer due to radiation

According to (Howell, Siegel, & Mengüç, 2010) practically all matter emits electromagnetic radiation. Thermal radiation transfer that takes place between two distant bodies depends on the difference between the fourth power of their absolute temperatures, according to Boltzmann's law (Howell et al., 2010). Solar radiation is an example of thermal radiation which is included in our ice model. Even at times when the solar radiation is negligible, thermal radiation still plays a role within the

model. For example the thermal radiation between the surface layer and the atmosphere remains non-negligible.

2.2 Effect of weather on ice growth

The weather conditions greatly influence which type of heat transfer dominates and which one becomes suppressed in the model. Consequently, other weather conditions besides outside temperature can influence ice growth. Hence, weather conditions which significantly affect the heat transfer should be accounted for in the model.

2.2.1 Precipitation

Precipitation may affect the conductive heat transfer. In this model, mainly the effect of snowfall will be investigated. A snow layer upon an ice layer 'separates' the ice layer from the atmosphere, effectively insulating the ice surface. Within the snow layer movement of air is restricted and therefore convective heat transfer is suppressed. Furthermore, the porous nature of snow results in a relatively low thermal conductivity within the snow layer (compared to the ice layer). The combination of suppressed convective and conductive heat transfer decrease the effect of the atmospheric temperature on the ice layer. Consequently, the ice layer's growth rate will decline.

2.2.2 Solar radiation

According to (Moene & van Dam, 2014) radiative fluxes as they are relevant to the ice model can be split on basis of their origin. Short-, and longwave radiation. They note that shortwave radiation is emitted from the sun, with a wavelength of 0.15-3 μm, and can be either direct or indirect after interaction with the atmosphere. Longwave radiation, on the other hand, is emitted by cooler objects (such as the Earth's surface and atmosphere), with a wavelength range of approximately 3-100 μm. The Earth's atmosphere plays an important role in determining the amount of radiation that reaches the surface, cloud coverage and the type of clouds are the most important causes of variation (Moene & van Dam, 2014). For this reason cloud coverage and solar radiation are investigated during the modelling phase.

2.2.3 Stability

Ice growth requires heat to flow out of the ice layer. In the case of a one dimensional ice layer, the heat can either flow into the water or into the atmosphere. In general, the water can't attain a lower temperature than the ice layer, or else the water would be ice itself. Also, heat flowing from the ice into the water would warm the water, which in turn would negate the ice growth. Consequently, the heat can only be released into the atmosphere. The air in the atmosphere has very poor conductive properties. The main way to transport heat within the atmosphere is through convection. The two driving forces behind the convection are wind and buoyancy.

Higher air temperatures correspond to a lower air density, hence a vertical temperature gradient of the air creates an airflow in the vertical direction. From now on heat flowing from the Earth's surface into the atmosphere will be addressed as the sensible heat flux (upwards positive). Initially, when the sensible heat flux is zero (and there is no wind velocity), layers of air are 'stacked' upon each other. Every

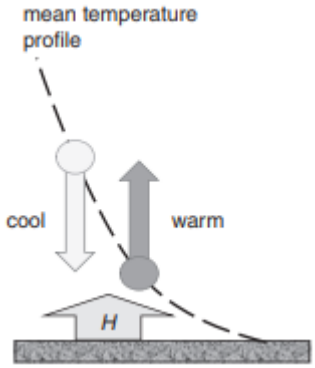

FIGURE 2.1: Relation between vertical air motion, temperature gradient and sensible heat flux (H) (Moene & van Dam, 2014)

layer with a different temperature and density. When heat is released from the ice layer into the air near the surface, the air starts to flow upwards, mixing the different air layers. On the other hand when, the sensible heat flux is either negative or very small, the initial 'stacked' layers return into the air due to density stratification; i.e., warm air will spontaneously rise and the cold air is relatively heavy and will stratify. In this case, the temperature measured at some height in the atmosphere can't reach the Earth's surface due to 'blockage' by underlying air layers, driven by buoyant forces. The freedom of the vertical air motion is addressed by the term 'stability'. Motion of air suppressed by buoyancy is defined as a stable condition, whereas free vertical motion is defined as an unstable (convective) condition (Moene & van Dam, 2014).

Due to solar radiation the temperature of the Earth surface rises. For surfaces like the Earth's soil, the rise of temperature creates a positive sensible heat flux. Along the same lines, during the night the sensible heat flux is usually negative, due to lack of solar radiation. By land, this mechanism causes variations between stability conditions during the diurnal cycle, being stable during the night and unstable during the day. Contrarily, when it comes to ice/water surfaces, the stability conditions don't follow the same pattern. When air temperatures are below zero, the temperature of the ice (being close to zero) is *higher* than the atmosphere's, causing a positive heat flux. During the day, the solar radiation either diminishes the positive surface heat flux or, in the case of ice melt, causes a negative surface heat flux. As a result, unstable conditions will likely appear during the night and near neutral/stable conditions generally appear during the day (over ice, over land it is reverse). The 'blockage' caused by the stably stratified conditions during ice melt, reduces the rate at which the ice melts, which may create an interesting asymmetry between the growing and melting stage of ice. This effect will be discussed in more detail later.

Chapter 3

Modelling ice growth

This chapter presents the ice growth model. The heat equation dictates, in the broadest sense, all the models. Therefore, a brief explanation of this equation is given. On the basis of the heat equation, several important assumptions (used for all the models) are established. Next, the base model is presented. Further complexity is then added through adopting various assumptions about physical factors involved.

3.1 The heat equation

The temperature profile over time within the ice is described by the solution of the classic heat equation:

$$\frac{\partial T}{\partial t} = -\alpha \nabla^2 T + Q(x, y, z, t) \tag{3.1}$$

T represents the temperature of the ice (in K), α is the thermal diffusivity of ice and Q an internal source term. The thermal diffusivity can be written as:

$$\alpha = \frac{k_i}{\rho_i c_i} \tag{3.2}$$

In which the thermal conductivity of ice is denoted as k_i (W/mK), the ice's density as ρ_i (kg/m^3) and it's heat capacity as c_i (kJ/kgK). Given any lake or canal, sources interacting with the system, like the atmospheric and water temperature, are assumed to be uniformly distributed along the horizontal plane. As a result, the horizontal temperature gradient in the ice layer is negligible compared to the vertical temperature gradient. This assumption simplifies the heat equation into:

$$\rho_i c_p \frac{\partial T}{\partial t} = -k_i \frac{\partial^2 T}{\partial z^2} + q(z, t) \tag{3.3}$$

Given any source, boundary conditions and an initial condition, equation (3.3) can be solved (both analytically and numerically).

3.1.1 Boundary conditions

Equation 3.3 requires two boundary conditions to solve. The boundaries are located at the surface of the lake (the top of the ice layer) and at the bottom of the ice layer. At the top layer heat needs to either escape or enter the ice in order for the ice layer to expand or contract respectively. At the lower boundary the temperature is assumed to be equal to the freezing point T_f (i.e 273.15 K or 0 Centigrade). The upper boundary is set to be at $z = 0$, with z downwards positive. The location of the lower boundary is not known, and is a distance $s(t) > 0$ (the ice thickness) away from the upper boundary.

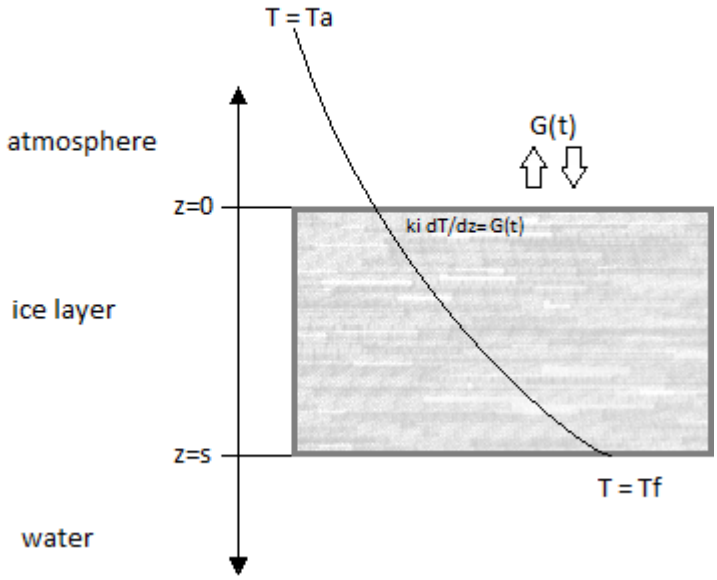

FIGURE 3.1: Schematic diagram of temperature profile and boundary conditions. Snowfall and heat flux coming from the water are neglected

Applying Fourier's Law to the upper boundary, the boundary conditions read:

$$k_i \frac{\partial T}{\partial z}(0,t) = G(t) \tag{3.4}$$

$$T(s(t),t) = T_f \tag{3.5}$$

In which G(t) represents the heat flux of the ice layer. G(t) is taken positive when heat enters the ice. At this time, the heat equation is not yet valid at the lower boundary. Apart from the initial condition, an additional condition is required to find the location of s over time. This additional condition is called the 'Stefan condition', named after the Slovenian physicist Josef Stefan. The Stefan condition evaluates the ice growth rate, which depends on the amount of heat added or withdrawn from the ice, divided by the latent heat of freezing and the ice's density. The Stefan condition thus reads:

$$\frac{\partial s}{\partial t} = -\frac{G(t) + Q_w(t)}{\rho_i L_f} \tag{3.6}$$

Where L_f (kJ/kg) represents the latent heat of freezing and Q_w the heat flux coming from the water (inwards the ice positive). Equation 3.6 lays the foundations of all upcoming ice models, as its solution describes the ice thickness over time.

3.2 The basic model

A few assumptions are made to start with a relatively straightforward model. First of all, the heat flux coming from the water (Q_w) is neglected. This transforms equation

3.6 into:

$$\frac{\partial s}{\partial t} = -\frac{G(t)}{\rho_i L_f} \tag{3.7}$$

The net heat flux at the surface of the ice layer (G) can be subdivided into two components: the sensible heat flux (H) and the net radiative flux (Q).

$$G(t) = Q(t) - H(t) \tag{3.8}$$

To preserve the conventions used in most literature, heat leaving the ice (heat flow in negative z direction) is taken negative for Q and positive for H. The radiation (Q) is assumed to be zero in the basic model, and will be implemented in later models. This leads to the following equation governing the basic model:

$$\frac{\partial s}{\partial t} = \frac{H(t)}{\rho_i L_f} \tag{3.9}$$

In the simplest case, our reference model, the surface temperature (T_s) is assumed to be equal to the temperature measured in the atmosphere (T_a). Later this (rather stringent) assumption is relaxed towards a more realistic assumption. Throughout the study 'steady state' conditions in the ice are considered; i.e., the temperature profile within the ice is assumed to be linear. The latter will be assumed for all the models. Implementing these assumptions into 3.4, 3.8 and 3.9 the ice growth rate is described by:

$$\rho_i L_f \frac{\partial s}{\partial t} = k_i \frac{(T_f - T_a(t))}{s} \tag{3.10}$$

Equation 3.10 is an ordinary differential equation which can be solved analytically for s. Given any initial ice thickness s_0 at t_0 and using the method of separation of variables, the analytic solution reads:

$$s(t) = \sqrt{s_0^2 + 2\frac{k_i}{\rho_i L_f} \int_0^t T_f - T_a(\tau) d\tau} \tag{3.11}$$

The values used for the physical variables can be found in table A.1. The density (ρ_i) and thermal conductivity (k_i) are slightly dependent on the temperature (see Table A.2). The changes caused by the temperature are in this case neglected and k_i and ρ_i are assumed to have a fixed value (see table A.1). The solution describes the thickness of the ice dependent on its initial state and the temperature in time. The basic model is therefore defined by equation 3.11.

3.3 Atmosphere-surface coupling

The basic model above assumes that $T_s = T_a$. In *reality*, however, T_a is usually measured at some level above the surface, with the air in between the surface and measurement height having a certain degree of resistance against the heat transfer. Therefore, as a first increase in model complexity, T_s is no longer assumed to be equal to T_a, but instead some function of T_a taking the air resistance into account. The heat resistance of the air depends on the local wind velocity and the stability of the system. Moene & van Dam (2014) present two equations describing the relation between the sensible heat flux, the temperature difference, the wind velocity and the stability condition (see section 2.2.3). For unstable conditions the relation reads:

$$\frac{H}{\rho_a c_p} \approx -\frac{\kappa^2 \Delta T \Delta u}{\ln\left(\frac{z_2}{z_1}\right)^2}(1 - 16Ri_{b*})^{\frac{3}{4}} \tag{3.12}$$

Where κ is the von Kármán constant (≈ 0.4), and z_1 and z_2 are the lower and upper heights respectively, at which the temperature is measured. ΔT is defined as T(z_2)-T(z_1) (in this case T_a-Ts) and Δu is defined in a similar fashion. ρ_a and c_p are the density and heat capacity of the air. Ri_{b*} is an effective bulk-Richardson number given by:

$$Ri_{b*} = \sqrt{z_2 z_1} \ln\left(\frac{z_2}{z_1}\right) \frac{g}{273.15} \frac{\Delta T}{\Delta u^2} \tag{3.13}$$

The gravitational acceleration constant is denoted as g (9.81 m/s^2).

In the stable case, equation 3.12 and 3.13 are no longer valid. In this case the following relation is given by (Moene & van Dam, 2014):

$$\frac{H}{\rho_a c_p} = \begin{cases} -\frac{\kappa^2 \Delta T \Delta u}{\ln\left(\frac{z_2}{z_1}\right)^2}(1 - 5Ri_b)^2 & \text{if } 0 < Ri_b < 0.2 \\ 0 & \text{if } Ri_b > 0.2 \end{cases} \tag{3.14}$$

With Ri_b given by:

$$Ri_b = (z_2 - z_1) \frac{g}{273.15} \frac{\Delta T}{\Delta u^2} \tag{3.15}$$

To properly approximate the surface temperature, z_1 needs to be close to the surface; i.e., close to zero (at the same time, z_1 can't equal zero as otherwise dividing by zero would occur). As z_1 approaches zero, the difference between the surface temperature and the observed temperature will approach zero as well. (Moene & van Dam, 2014) provide several heights z_0, depending on the surface composition, that meet the requirement $T(z_0) \approx T_s$. These heights are called the aerodynamic roughness lengths. In this study, a homogeneous surface is assumed. In reality, the roughness length can vary due to, for example, local vegetation.

TABLE 3.1: Typical values for aerodynamic roughness lengths for natural surfaces (Moene & van Dam, 2014)

Surface	**Remark**	z_0
Water	Still-open	$10^{-4} - 10^{-3}$
Ice	Smooth sea ice	10^{-5}
Ice	Rough sea ice	$10^{-3} - 10^{-2}$
Snow		$10^{-4} - 10^{-3}$
Soil		0.002

Table 3.1 gives an indication of the order in which the roughness lengths typically lie. Taking $z_1 = z_0$, H (in equations 3.12 and 3.14) will depend on T_s. Applying 3.4, 3.8, 3.12, 3.14 and the assumption that the temperature profile within the ice is linear, an expression for T_s can be found by solving the following for T_s:

$$k_i \frac{T_f - T_s}{s} = \begin{cases} -\rho_a c_p \frac{\kappa^2 (T_a - T_s)\Delta u}{\ln\left(\frac{z_2}{z_1}\right)^2}(1 - 5Ri_b)^2 = f(T_s) & \text{for stable conditions} \\ -\rho_a c_p \frac{\kappa^2 (T_a - T_s)\Delta u}{\ln\left(\frac{z_2}{z_1}\right)^2}(1 - 16Ri_{b*})^{\frac{3}{4}} = g(T_s) & \text{for unstable conditions} \end{cases} \tag{3.16}$$

In both the stable and the unstable case the (effective) bulk-Richardson number influences the validity of the equation 3.16. When the bulk-Richardson number grows too large, the right-hand side of equation 3.16 will either become zero or contain imaginary values. The equations 3.12 - 3.15, are usually applied under the condition that $z_2/z_1 < 6$. Because $z_1 \to 0$ (to approximate T_s), the condition won't be met in this case. Consequently, the magnitude of the (effective) bulk-Richardson number will increase significantly, causing the Richardson number to become unreliable during calculations. To avoid this undesirable situation, both cases in equation 3.16 are linearised into a first degree Taylor polynomial centred at $T_s = T_a$:

$$k_i \frac{T_f - T_s}{s} = \begin{cases} f(T_s) = f(T_a) + \frac{f'(T_a)}{1!}(T_s - T_a) = W(\Delta u)(T_s - T_a) & \text{(stable)} \\ g(T_s) = g(T_a) + \frac{g'(T_a)}{1!}(T_s - T_a) = W(\Delta u)(T_s - T_a) & \text{(unstable)} \end{cases} \tag{3.17}$$

With $W(\Delta u)$ being a coefficient depending on the wind velocity:

$$W(\Delta u) = \frac{\rho_a c_p \kappa^2 \Delta u}{\ln\left(\frac{z_2}{z_1}\right)^2} \tag{3.18}$$

When linearised around T_a, both cases in equation 3.16 lead to the same result. The result does no longer meet the stability requirements, but describes the atmospheric heat resistance in *neutral* conditions. Solving equation 3.17 for T_s results in:

$$T_s = \frac{W(\Delta u) T_a s + k_i T_f}{W(\Delta u) s + k_i} \tag{3.19}$$

To finalise the solution, equation 3.19 is substituted into 3.10. The resulting differential equation being dependent on T_a and the wind velocity Δu. The equation reads:

$$\rho_i L_f \frac{\partial s}{\partial t} = k_i \frac{(T_f - T_a(t))}{s + \frac{k_i}{W(u)}} \tag{3.20}$$

To solve 3.20 analytically, another condition is required: the wind velocity must be constant during the entire time span; i.e., $W(\Delta u)$ is a constant. The analytical solution in that case becomes:

$$s(t) = \sqrt{s_0^2 + 2\frac{k_i}{\rho_i L_f}\int_0^t T_f - T_a(\tau)d\tau + \left(\frac{k_i}{W(u)}\right)^2} - \frac{k_i}{W(u)} \tag{3.21}$$

The heat capacity and density of the atmosphere are dependent on the temperature of the atmosphere (see Table A.3) In this model the density and heat capacity are assumed to be constant and have a value of 1.22 (kg/m^3) and 1.0 (kJ/kgK) respectively.

To solve 3.20 considering fluctuating wind velocities (in time), numerical methods are required.

As stated before, the final equations containing atmospheric coupling (equation 3.20 and 3.21) do not include the effects of stability. To implement stability into the model, a second degree Taylor expansion is required, combined with knowledge of the stability conditions. The stability (at a given time) could be determined using iterative methods. Those methods are purposely left out in this study, since iterative processes require relatively high computational time. At first, neglecting the stability altogether was not intended, as the initial idea was to implement stability directly by using equations 3.12-3.15.

3.4 Radiation

Up to now, thermal radiation $Q(t)$ has been neglected and assumed to be zero. Thermal radiation is divided into two categories: longwave radiation (L) and shortwave radiation (K). Since both types are expressed in W/m^2, the energy balance at surface reads:

$$Q = L^+ - L^- + K^+ - K^- \tag{3.22}$$

The '$+$' sign indicates energy entering the system (downwards), whereas the '$-$' sign indicates energy leaving the system. In this model, solar radiation is assumed to be the only source of incoming shortwave radiation (K^+). During the diurnal cycle, this means the incoming shortwave radiation is relatively high during the day and (in general) negligible during the night. During the night the net radiation is thus solely dependent on the longwave radiation leaving the ice and entering the ice from the atmosphere. Depending on the surface properties, the incoming solar radiation is partially reflected, resulting in outgoing shortwave radiation (K^-). The percentage of the solar radiation that gets reflected is called the surface's albedo (α).

Longwave radiation is emitted from the ice into the atmosphere and vice versa. The Stefan-Boltzmann law describes the energy radiated by an arbitrary body as follows:

$$L_j = \epsilon_j \sigma T_j^4 \tag{3.23}$$

The subscript 'j' represents the different bodies, in this case the atmosphere and the surface. The constant ϵ is called the emissivity, which is dependent on the properties of the body. σ ($\approx 5.670 \times 10^{-8} Js^{-1}m^{-2}K^{-4}$) is the Stefan-Boltzmann constant, a constant derived from other physical constants. It is important to note that the temperature (T) is the thermodynamic temperature, given in Kelvin. In the previous models, both the Kelvin and the Celcius temperature scale could be used, because those models only dealt with temperature *differences*.

The emissivity of the atmosphere depends largely on the cloud coverage and water vapour. In the case of a clear sky, the water vapour is the most active constituent. The emissivity $\epsilon_{a,clear}$ is then approximated by the following equation (Moene & van Dam, 2014):

$$\epsilon_{a,clear} = c_1 + c_2\sqrt{e_a} \tag{3.24}$$

Where e_a is the water vapour pressure (hPa), and c_1 and c_2 are empirical constants with standard values of 0.52 and 0.065 $\text{hPa}^{-\frac{1}{2}}$. Interpolating the clear sky

emissivity and the emissivity of clouds (assuming a cloud to be black radiator with emmisivity of 1), results in the atmospheric emissivity (Moene & van Dam, 2014):

$$\epsilon_a = f_{cloud} + (1 - f_{cloud})\epsilon_{a,clear} \tag{3.25}$$

f_{cloud} is the cloud fraction i.e. the percentage of cloud coverage. Assuming the albedo and emissivity of the surface are given, all the necessary equations are now available in order implement radiation into the model. Equation 3.22 now reads:

$$Q = \epsilon_a \sigma T_a^4 - \epsilon_s \sigma T_s^4 + (1 - \alpha)K^+ \tag{3.26}$$

ϵ_s is the emissivity of the surface, in this case the emissivity of ice. Since equation 3.26 contains T_s (which is unknown), equation 3.4 needs to be solved for T_s in terms of T_a (in a similar fashion as in the case of atmosphere-surface coupling). To further simplify the calculations, T_s is linearised into a first degree Taylor polynomial centred at $T_s = T_a$. This results in the following equation describing Q:

$$Q = (\epsilon_a - \epsilon_s)\sigma T_a^4 - 4\epsilon_s \sigma T_a^3 (T_s - T_a) + (1 - \alpha)K^+ \tag{3.27}$$

T_s can be solved for by combining equation 3.4, 3.8. Substituting for T_s into equation 3.10 (including surface-atmosphere coupling) gives:

$$\rho_i L_f \frac{\partial s}{\partial t} = \frac{k_i}{s}(T_f - \frac{s(\epsilon_a + 2\epsilon_s)\sigma T_a^4 + sW(u)T_a + s(1 - \alpha)K^+ + k_i T_f}{3s\epsilon_s \sigma T_a^3 + sW(u) + k_i} \tag{3.28}$$

Supposing K^+ is a given value in time, equation 3.28 can be solved numerically. The solution renders the ice thickness in time, including radiation and surface-atmosphere coupling.

3.5 Precipitation

Precipitation can influence the ice growth in several ways. This study only looks into the effects of snowfall. The porous nature of snow layers has an important thermodynamic consequence: the snow layer's thermal conductivity is relatively low, compared to the ice's conductivity. Consequently, a snow layer covering the ice can significantly reduce the ice growth rate. The snow density varies in time due to the snow's own weight (which causes it to compress), and due to subsequent freezing/thawing cycles which causes ice crystals to lose their 'open' shape. Since the density affects the thermal conductivity, the conductivity also is time dependent. Another important factor influencing the ice growth rate, is the height of the snow layer. Logically, the compression of the snow in time directly relates to the height of the snow layer. The FLake model, an ice thickness model supplied by the Leibniz Institute of Freshwater Ecology, provides an elegant empirical solution to the snow conductivity (De Bruijn et al., 2014):

$$k = k_{snow} + (k_{ice} - k_{snow})e^{-5h} \tag{3.29}$$

Where h represents the height of the snow layer. In the FLake model the snow density is assumed to not vary in time, but being a constant $\rho_{snow} = 320 kg/m^3$ instead. As a result of the constant density, the conductivity of the snow, k_{snow}, remains constant as well. The effective conductivity k of the snow and ice layer combined,

can now be calculated using equation 3.29. By replacing k_i for k in the previous models, snow is now taken into account.

Apart from the low thermal conductivity, in some cases the higher surface albedo of snow also plays a role in diminishing the ice growth rate. The surface albedo varies along with the state of the ice and snow. For example, when ice melts the albedo reduces. In order to maintain simplicity, even though variation in albedo can significantly affect the ice growth, two fixed values are taken for the snow and ice albedo.

3.6 Water temperature

Water temperature below the lower boundary (the bottom of the ice layer) is higher or equal to the temperature of the lower boundary itself (T_f). Similar to the atmosphere, the water experiences a density gradient caused by temperature differences within the water. Water has its highest density at approximately $4°C$ (De Bruijn et al., 2014). The temperature at the bottom of the lake T_b is therefore assumed to be equal to $4°C$. The heat flux from the water, entering through the bottom of the ice layer, is determined by applying Fourier's Law. Assuming the temperature gradient of the water is close to linear, the heat flux caused by water temperature (Q_w) is estimated by:

$$Q_w = k_w \frac{T_b - T_f}{D - s} \tag{3.30}$$

With k_w being the thermal conductivity of water and D the total water depth ($z_{bottom} - z_{surface}$). Because the movement of water is assumed to be non-turbulent, k_w is an absolute minimum. In reality this assumption will hold in most cases, since generally little turbulent movement of water occurs in channels and lakes (except when water structures like for example locks are present). Also, the water will be stably stratified (which suppresses turbulence). The depth of the observed lakes fluctuate around approximately 2 meters. The bottom temperature is assumed to be $4°C$, since the water has the highest density around this temperature (see Table A.4). The thermal conductivity of water is assumed to be around 0.606 W/mK. The water heat flux, can be implemented into the models using equation 3.6.

Chapter 4

Results

In this chapter the effects of different weather conditions are investigated. First an academic sensitivity study is performed. This means that different scenarios are calculated in which the ice model is forced by artificial ice data ('what if' scenarios). Second, actually occurred cases will be studied. Here the model is forced with historical weather data and ice growth is compared with actually observed growth during those periods.

4.1 Model sensitivity analysis

In order to properly understand in which way all the parameters affect the model, the ice thickness is predicted on the basis of an idealised data set. By controlling the parameters in the data set, the effect of different parameters on the ice growth can be visualised. This in turn gives a better understanding of the significance of certain weather phenomena.

To properly see the effects between the growing and melting stage of ice, a symmetrically odd function describing the temperature profile is assumed, in this case a negative sine wave (in order to start with ice growth, the initial temperature, and therefore the sine, needs to be negative). The period is set to one hundred hours and the amplitude to $10°C$. This temperature distribution is far from realistic, but the large period combined with rather extreme amplitudes result in high freeze/thaw rate, enlarging the effects of the investigated parameters. At last, to minimise the numerical errors, an initial ice thickness is assumed (5cm). This temperature profile and initial ice thickness is assumed in all the simulations.

In figure 4.1 the resulting ice thickness due to various wind velocities is plotted using the surface-atmosphere model, visualising the effects of different wind velocities (neglecting radiation). The rather unrealistic maximum ice thicknesses are the result of a relatively high amplitude and the long period of freezing (fifty hours of uninterrupted subzero temperatures). Another way to influence the atmosphere-surface coupling is to change the roughness length (z_0). The effects of these changes are represented in figure B.9. Increasing the wind velocity positively affects both the growth and melt rate of the ice. A higher wind velocity results in a higher maximal ice thickness, yet the final ice thickness remains the same regardless of the wind velocity. The symmetry was initially not expected, and is caused by the absence of stability in the atmospheric coupling equations (3.20 and 3.21). Mathematically, an infinite wind velocity would result in T_a to be equal to T_s, and result therefore into the basic model equation (3.11).

To look into other parameters, the wind velocity is now fixed to 5 m/s. To investigate certain cases of radiation, the solar radiation is assumed to be zero for now. As mentioned earlier, this is far from realistic, as hundred hours without sun is extremely unlikely. The emissivity of ice is a fixed value of 0.96. The absence of solar

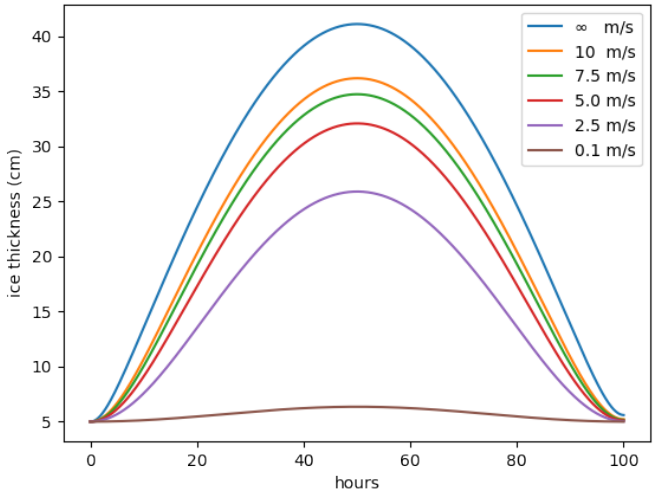

FIGURE 4.1: Ice thickness profile for various wind velocities and the basic model.

radiation renders the albedo irrelevant at this point. Now, the effects of the atmosphere's emissivity can be visualised by alternating the amount of cloud coverage (see figure 4.2).

The cloud coverage dampens the ice growth in general and increases the melt rate. Interestingly, including radiation into the model removes the symmetry between the ice growth and melt, decreasing the influence of the atmospheric temperature during the melting stage.

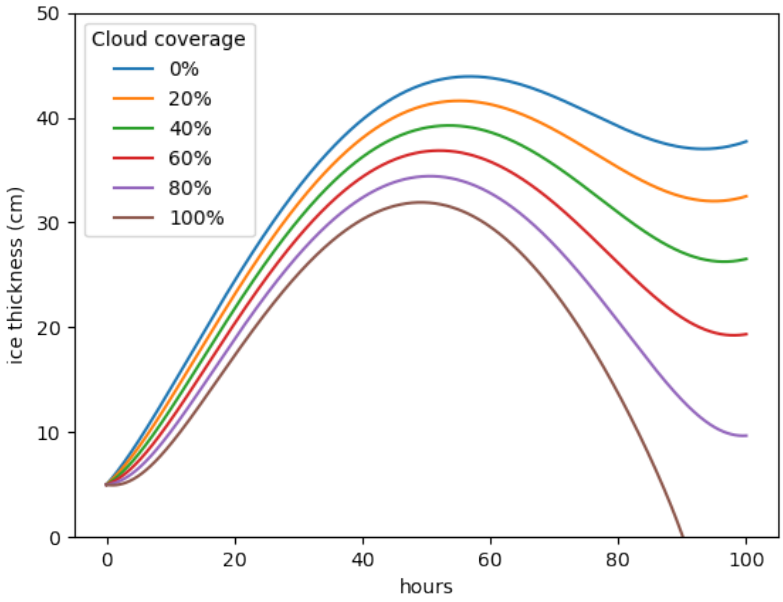

FIGURE 4.2: Ice thickness profile for various cloud coverage percentages with a fixed wind velocity of 5 m/s.

This results contradicts the expectation that adding radiation to the system would

lead to an increased melt rate (in all cases). The net longwave radiation leaving the ice's surface will, in fact, increase ice growth. It should be noted that this case is unrealistic as well: In reality high percentages of cloud coverage would suppress the (in this case relatively high) temperature amplitude.

The surface temperature depends on the net radiation, regardless of the source (whether it's longwave or shortwave). For that reason solar radiation has basically the same effects as cloud coverage, because both influence the net radiation. Regardless of the similar effects, the solar radiation is looked at independently, such that the effects of certain *quantities* of solar radiation can be expressed. The solar radiation unit is set to J/cm^2, the same unit used in the weather data sets provided by the KNMI. To investigate which amounts of solar radiation affect the ice growth significantly, the cloud coverage is now fixed at 40%. Varying the albedo or the solar radiation itself has the same effects as they are inversely proportional. In this case the albedo is given a fixed value of 80% and the solar radiation is varied along different plots (see figure 4.3). The differences are already visible at 20 J/cm^2, and become more significant as the amount of radiation increases.

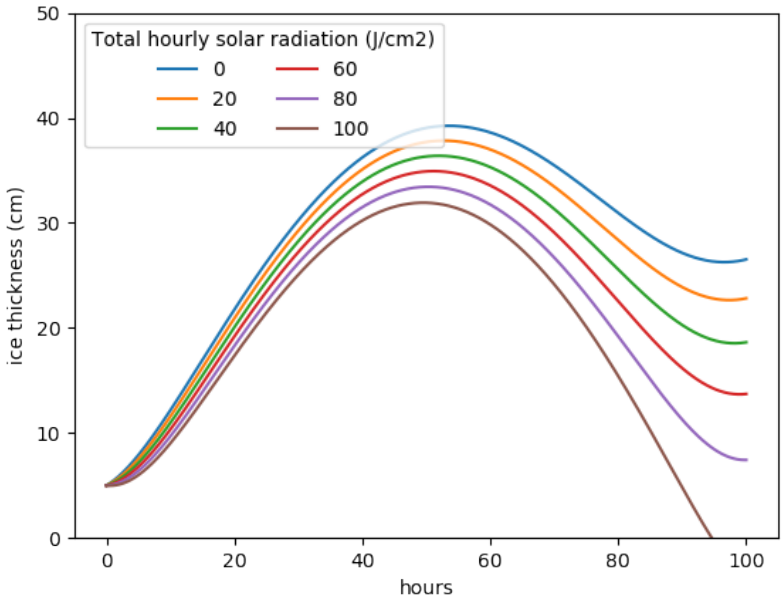

FIGURE 4.3: Ice thickness profiles with varying intensity of solar radiation.

Finally, the consequences of snowfall are visualised. All previous variable parameters are fixed, in this case is the solar radiation set at 80 J/cm^2. The effects of snowfall are divided into two cases: snowfall during the ice growth stage and snowfall during the melting stage. The two different cases are plotted with different snow depths. During the ice growth stage, the snowfall is assumed to fall between the 15th and 35th hour, whereas during the melting stage the snow falls between the 65th and 85th hour. The thermal conductivity of (dry) snow lies between 0.05 and 0.25 W/mK (Engineering ToolBox, 2003a). In this case the conductivity is fixed at 0.25 w/mK. The surface albedo of (dry) snow is estimated to be around 0.95. Figure 4.4 visualises the response of the model to snowfall during ice growth.

The snow layer reduces the ice growth significantly. Increasing the height of the snow layers results in a decrease of the growth rate. During the melting stage the

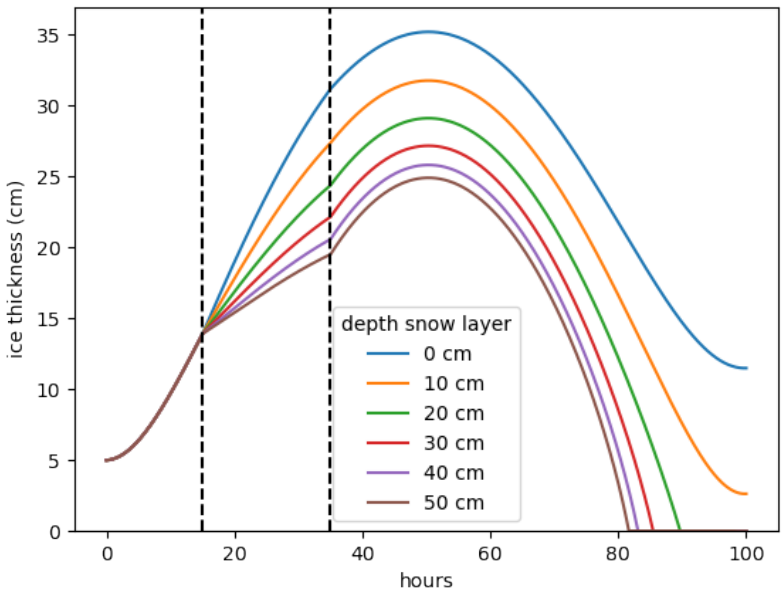

FIGURE 4.4: Ice thickness profiles with varying snowfall during the ice growth stage. The dashed lines indicate the range in which snow was present.

snow layer affects the model as is presented in figure 4.5. The snow layer reduces the melt rate as well. Similarly to snow layers during the growth stage, the melt rate decreases with an increase of the snow layer's height. The fact that the ice experiences any growth or melt at all when covered by a 50cm snow layer, can be explained by the extreme temperature amplitude and freezing time-period.

From this paragraph, studying modelling sensitivity for a (rather extreme) case, it can be concluded that all the investigated meteorological parameters influence the ice growth. Wind improves the atmospheric heat transport, radiation can both positively and negatively influence ice growth and snow layers decrease the ice growth/melt rate. In the next paragraph, model outcomes will be compared to more realistic cases.

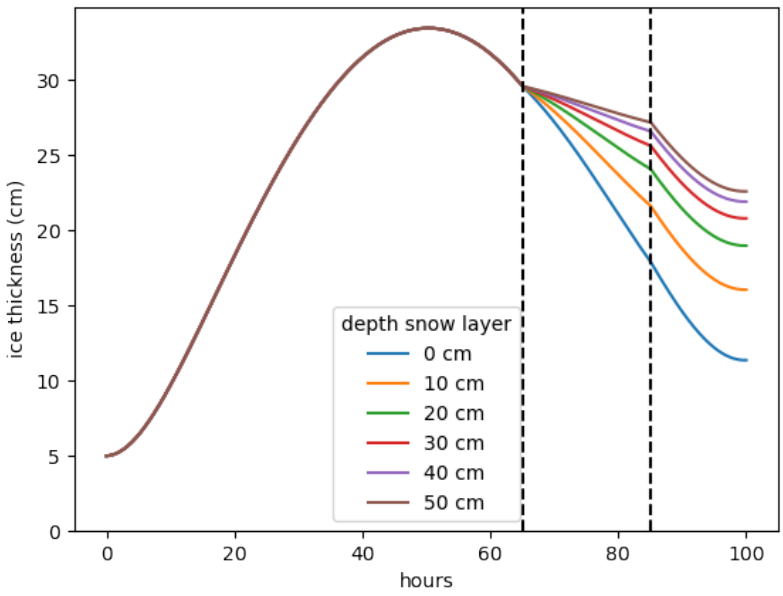

FIGURE 4.5: Ice thickness profiles with varying snowfall during the ice melting stage. The dashed lines indicate the range in which snow was present.

4.2 Comparison to historical weather data

Three different data sets are used to study ice growth under realistic conditions. Two of those provide the observed ice thickness in several lakes in the province Friesland (The Netherlands), in the years 2010 and 2012. The third data set presents the water temperature at several depths of a lake/ditch in the region near Cabauw (The Netherlands) in 1997. The ice thickness of the models forced with contemporary weather data provided by The Royal Netherlands Meteorological Institute (KNMI) is compared to the ice thickness of the observed data sets for that period. In the case of the data sets regarding the province of Friesland, weather data measured in the city Leeuwarden is used. The observed ice thicknesses of the Friesland data sets are paired with the geographic coordinates of the measurement's place. Using reverse geocoding the data sets are distinguished into different lakes, each with its own ice thickness.

As can be seen in figure 4.6, the observed ice thicknesses at fixed times varies with location within Friesland, especially in 2010. The variation is likely caused by different weather- and environmental conditions between locations, e.g. difference in microclimate. By using only weather data originating from Leeuwarden, the difference in microclimate throughout Friesland can not be accounted for. For that reason, the focus of the comparison between the Friesland data in 2010 and the models will primarily be on their shape and whether or not the model lies within the data spread. The relatively minimal spread in 2012 can be explained by a higher consistency regarding the observed locations, compared to the 2010 data.

For the Cabauw data set, the water temperatures measured at several depths needs to be translated into ice thickness. A linear approximation of the water temperature along the depth is made, with the use of the known water temperatures at several depths. The depth at which the linearly approximated temperature reaches

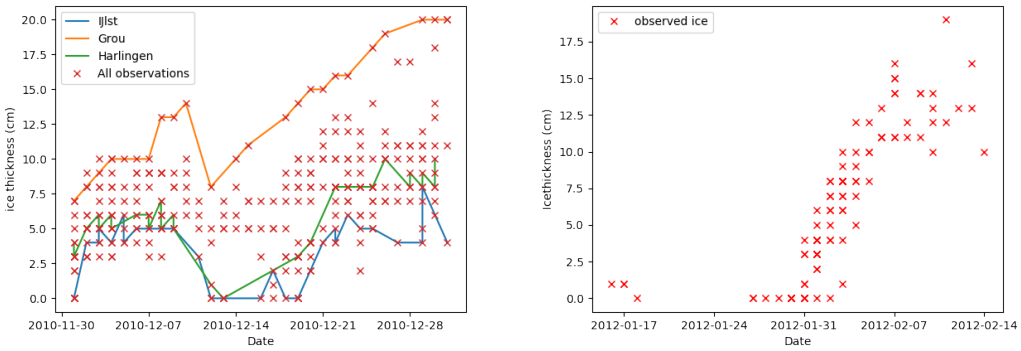

(a) Friesland 2010 (b) Friesland 2012

FIGURE 4.6: Ice thickness: all observation and a few examples of specific lakes in Friesland during 2010 (a) and all observations in Friesland during 2012 (b).

the freezing point, is taken as the ice thickness. During the melting of ice, convective processes cause stably stratified water layers to mix. Assuming a linear temperature profile in the water does no longer hold in that case, causing the method of (linearly) approximating the ice thickness to not be viable during the melting of ice. Therefore, during the melting stage a large part of the data is left out. The estimated ice thickness is visualised in figure 4.7 (b).

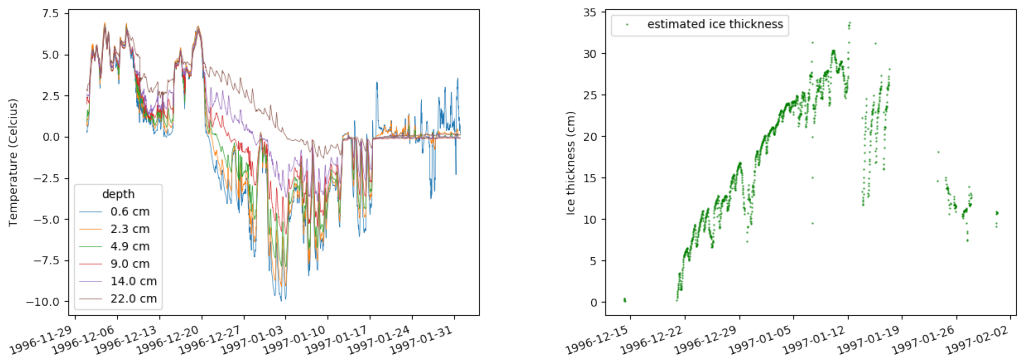

(a) Cabauw water temperature (b) Cabauw ice thickness

FIGURE 4.7: The water temperature measured at several depths in a lake in cabauw (a) and its estimated ice thickness (b)

The available ice thickness data is now compared with the ice prediction model. The reason these results aren't presented at the start of this chapter, is because this concerns the primary modelling phase (further improvement is required in subsequent studies). The visualisation of the models in detail can be found in Appendix B. The basic model is solved analytically using equation 3.11. The blue lines in figures 4.8, 4.9, and 4.10 represent the basic model. In all cases the basic model (equation 3.11) overestimates the ice thickness. As mentioned in section 3.2, this overestimation can be explained by the assumption that $T_a = T_s$. The error and correlation between the prediction and observations are calculated using the **daily mean** of the

observations and predictions. This way, further complications due to different sample sizes is prevented. Henceforth, when mentioning errors and correlations, the actual errors and correlations relate to the mean of contemporary data. The error is determined using the Root Mean Squared Error (RMSE). In the case of the basic model, the error ranges from 10.45cm to 12.59 cm. The correlation is calculated using the Pearson correlation coefficient. The correlation coefficient of the basic model ranges from 0.82 to 0.93, indicating a strong positive correlation. So with the most basic model (equation 3.11) a strong correlation but also a strong bias is found, indicating that the model is incomplete.

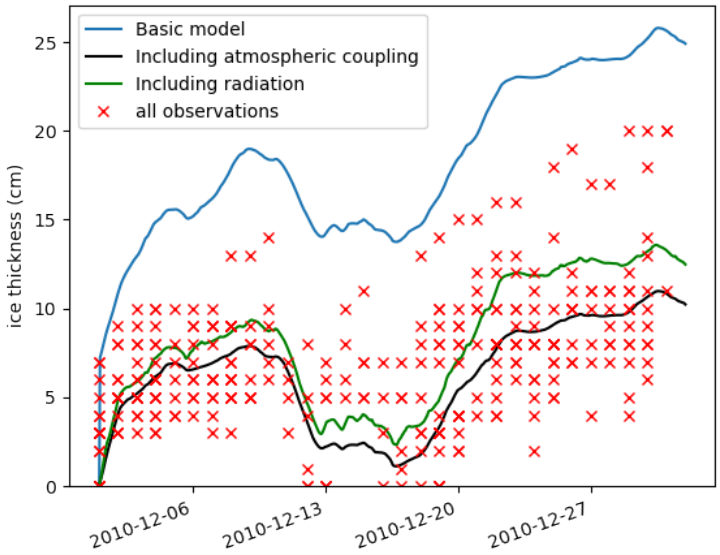

FIGURE 4.8: Predicted ice thickness in Friesland 2010 including the meteorological parameters: atmospheric coupling and radiation

The correlation coefficient and RMSE are given for all cases in table 4.1.

TABLE 4.1: The RMSE and correlation of the models compared to the observed data

	Friesland 2010		Friesland 2012		Cabauw 1997	
	RMSE (cm)[1]	Corr.	RMSE (cm)	Corr.	RMSE(cm)	Corr.
Basic model	10.42	0.82	12.59	0.93	10.45	0.83
Including atmospheric coupling	2.02	0.82	3.12	0.98	5.01	0.82
Including radiation	2.19	0.83	6.15	0.98	-	-

Next, the exchange between the atmosphere and the surface is (partially) accounted for. Due to the implementation of realistic atmospheric coupling, T_s is expected to increase compared to the reference model ($T_s = T_a$, equation 3.11). This should lead to a decrease of the temperature gradient in the ice layer. Using the governing equation 3.20, and the wind velocities given by the data sets, the model can be solved numerically. Numerical solutions are provided by using the forward Euler method combined with time steps of one hour. These numerical solutions are presented in the figures 4.8, 4.9, and 4.10 as the black lines. This time, the model

[1]The spread of 2010 data is too large to draw quantifiable conclusions in terms of RMSE.

no longer overestimates the ice growth and the results appear to lie within the data spread instead. This also explains the significant decline of the RMSE, compared to the basic model. As shown in table 4.1, the RMSE ranges from 2.02 cm to 5.01 cm, whilst the data remains strongly correlated.

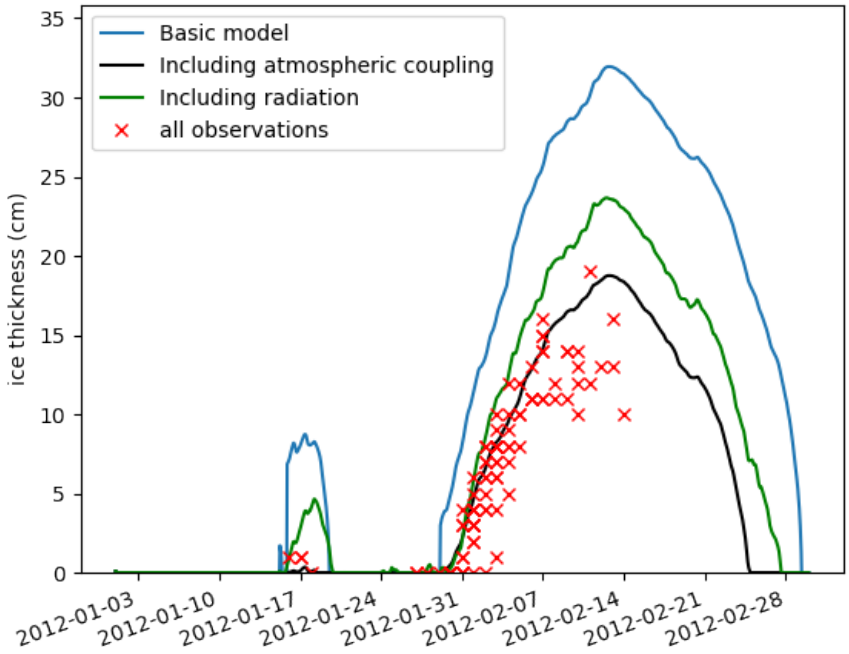

FIGURE 4.9: Predicted ice thickness in Friesland 2012 including the meteorological parameters: atmospheric coupling and radiation

The Friesland data sets only measure whether or not snowfall took place, not the amount of snow that has fallen. Therefore precipitation is not included in this model. That leaves radiation and the water temperature as the remaining parameters which can be implemented into the model. The radiation can be implemented using equation 3.28. The water's negative effect on ice growth, is inserted into the model using equation 3.6. Similar to the wind velocity, the (hourly) incoming global radiation and the cloud coverage is given by the data sets. The model is solved numerically, resulting green lines in figures 4.8 and 4.9. An increase of ice thick growth compared to atmospheric coupling model is found. Physically, this would mean that the net radiation at the ice's surface generally turned out to be negative (heat leaving the ice). This implies either that the cloud coverage or the solar radiation was relatively low during the time period. This would physically make sense, because a low cloud coverage would result in little atmospheric longwave radiation entering the ice, decreasing the net radiation at the surface. The RMSE increases compared to the case without radiation and the correlations remains nearly the same. The model still estimates the ice thickness rather accurately.

Even though the model is physically more accurate, the result is less accurate. The reason why the model's accuracy decreases, should be investigated further. The absence of stability in the models could explain the overestimation of the radiation models (green lines in figure 4.8 and 4.9), yet also the underestimation of the atmospheric coupling model (black line) in figure 4.10.

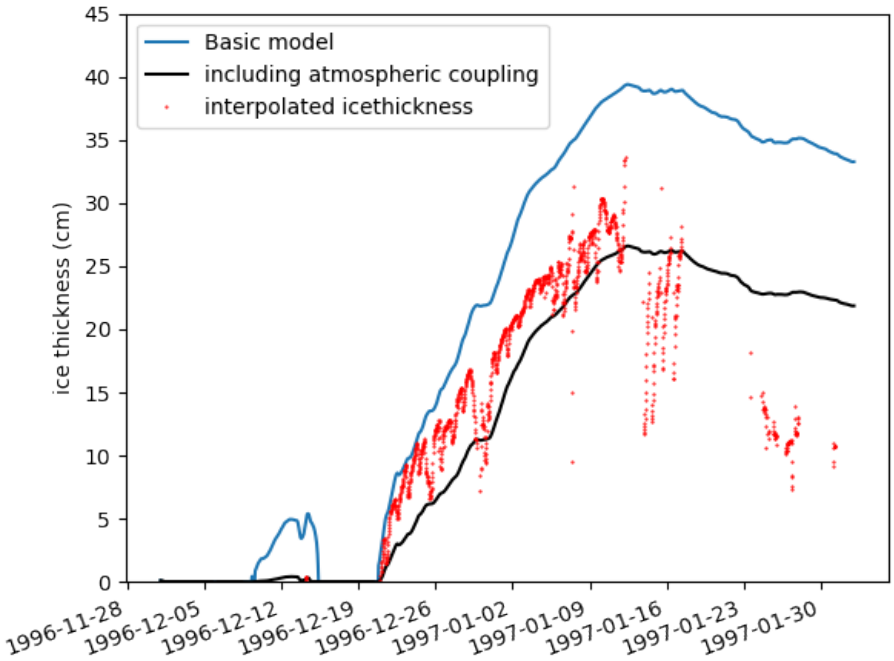

FIGURE 4.10: Predicted ice thickness in Cabauw 1997 including the meteorological parameter: atmospheric coupling

Including water sources to the model result in the same green lines in figures 4.8 and 4.9, rendering the water source negligible. The Cabauw data can not be modelled with inclusion of radiation, as the data from 1997 does not contain cloud coverage at all.

Chapter 5

Discussion

This chapter discusses the results obtained from the models. First, the effects of different weather conditions are reviewed. Afterwards, the validity of the historical weather data models are discussed.

5.1 Sensivity analysis

The idealised weather conditions (figure 4.1-4.5) give an insight of the effects of several meteorological parameters. Increasing wind velocities and roughness lengths clearly stimulate the ice growth/melt rate of the ice layer. This can be explained by the fact that the wind increases the 'effectiveness' of the heat transport across the atmosphere. When the wind velocity approaches infinity, the model converges to the basic model. Constant wind velocity does not create any asymmetry across the melting and growing stage of ice. The rippling of the water surface, caused by the wind, would increase the ice growth (z_0 increases). This is not taken into account in the models.

Solar radiation and cloud coverage impact the net radiation at the surface. This change in net radiation across the surface causes an asymmetry between the growing and the melting stage of ice. The ice melt rate decreases while the growth rate increases. Both the cloud coverage and solar radiation negatively influence this process; i.e, an increase of either cloud coverage or solar radiation increases the melt rate and decreases the growth rate compared to the case where the sky is clear and no solar radiation reaches the surface. The effects of solar radiation are already visible at an hourly intensity of 20 J/cm^2, and become more significant as the amount of radiation increases.

Snow layers isolate the ice layers from the atmosphere. The low thermal conductivity of the snow layers cause the ice growth/melt rate to decrease. Large amount of snowfall can even halt the ice growth completely. Difference between ice growth and melt is not apparent in this model. This does not imply there are no differences, as in reality the physical properties of the snow layer (for example the albedo) changes between melting and fresh snow.

5.2 modelling the historical weather data

Due to the spread of the observed ice thickness data, the validity of the models can't be determined precisely. Even though the accuracy of the models can't be determined exactly, several results still stand out. The basic model (fig 4.8-4.10) overestimates the ice thickness for all the data sets. This physically explained by the fact that T_a is assumed to be equal to T_s. This also explains the relatively high RMSE (table 4.1). The high correlation suggests that the shape of the base model curve is

very similar to the (mean) observed ice thickness curve. The similarity, in absence of other meteorological parameters apart from temperature, suggests that the temperature indeed plays a dominant role in forming the prediction curve's shape.

By inclusion of a more realistic description of heat transfer within the atmosphere, the models approach the observed ice thicknesses (figure 4.8-4.10). The correlation remains nearly the same (compared to the correlation with the basic model), suggesting that the atmospheric heat resistance doesn't influence the curve's shape. This model approximates the observed ice thickness fairly well, as indicated by the low RMSE (table 4.1).

Including radiation, the models' results lie within the observed data spread, upholding approximately the same shape in time as the previously discussed cases, as shown in figure 4.8-4.10. The RMSE increases compared to the model with only atmospheric heat resistance included. In this case the inclusion of radiation has therefore a negative (unwanted) effect on the predictive power of the model. Logically, this makes no sense, as the model grows in physical accuracy. This may imply that compensating errors have been made in the modelling process, and hence further research concerning this aspect is required.

The difference of ice thickness between lakes within the same data set can be caused by spatial variations between meteorological parameters. For example, local temperature differences influences the local ice's growth/melt rate. Also, other circumstances can play an important role, like, for example, local vegetation within and around the lakes, human/animal interaction with the lake and the initial flow velocity of the lake. These parameters are not taken into account in the models.

The models are constructed under the assumption that only vertical components affect the ice thickness whilst in reality the environment can influence the ice thickness from all directions. This contributes to the error of the models as well.

Chapter 6

Conclusions and recommendations

6.1 Conclusions

The effects of a variety of meteorological parameters have been investigated. This study focused on the following parameters: temperature, air resistance to heat, precipitation, radiation and stability. The latter is a phenomena causing 'blockage' of the heat transfer from the atmosphere to the surface due to stratification of the air. The study yields the following results:

1. The difference between the measured temperatures at 1.5m and the surface is non-negligible. The air's heat resistance reduces the ice growth rate.
2. Assuming an initial ice layer, high wind velocities above the ice layer increase the ice growth rate. The wind increases the effectiveness of heat transport between the surface and the atmosphere.
3. While solar radiation decreases ice growth (due to warmer temperatures), the net effect of including radiation in the ice growth model can be both positive or negative, depending on the sign and magnitude of the longwave radiation. The inclusion of radiation also creates an asymmetry between the melting and growing of ice (ice grows faster and melts slower).
4. Cloud coverage, though coherent with radiation, can impact the ice growth significantly: large coverage percentages decrease the ice growth and increase the ice melt.
5. Realistic values of solar radiation dampen the effects caused by cloud coverage; i.e., the magnitude of the net radiation at the surface drops.
6. Accumulation of a snow layer reduces the ice growth rate, both in the melting and the growing stage.
7. Heat coming from the water is negligible, and does not significantly delay the growth of ice.

6.2 Recommendations

The (primary) models gave an encouraging estimation of the ice thickness. In the future, it is advised to look further into the effects of the meteorological factors, in order to find out why inclusion of radiation lead to unwanted effects. Also, more data sets are required to check whether or not the model can be applied universally. This study is aimed at retaining a low complexity compared to increasing the accuracy at the cost of a high complexity.

To further improve future models, including all parameters mentioned above (temperature, air resistance to heat, precipitation, radiation and stability) is recommended. Better understanding of the relative impact of these meteorological parameters, could explain the reason radiation impacts the predictive power negatively in this study, possibly as a consequence of compensating errors by other meteorological parameters. Also, the difference of snowfall during the melting and growing stage, should be looked into further.

Appendix A

Various physical properties

TABLE A.1: The values used for the variables in the model

Variable	Value	Unit	Description
D	2	m	Water depth
c_p	1.0	kJ/kgK	Heat capacity air
g	9.81	m/s^2	Gravitational acceleration
k_i	2.22	W/mK	Thermal conductivity ice
k_s	0.25	W/mK	Thermal conductivity snow
k_w	0.606	W/mK	Thermal conductivity water
L_f	334	kJ/kg	Latent heat of freezing
T_a	-	K	Temperature atmosphere
T_b	277.15	K	Temperature bottom of lake
T_f	273.15	K	Freezing point
T_s	-	K	Temperature surface
u	-	m/s	Wind velocity
z_0	10^{-3}	m	Roughness length
z_1	10^{-3}	m	Lower measuring height
z_2	1.5	m	Upper measuring height
α_i	0.6	-	Albedo ice
α_s	0.95	-	Albedo snow
ϵ_a	-	-	Emissivity air
ϵ_s	0.96	-	Emissivity ice
κ	0.4	-	von Kármán constant
ρ_a	1.22	kg/m^3	Density air
ρ_i	916.2	kg/m^3	Density ice
σ	5.670×10^{-8}	$Js^{-1}m^{-2}K^{-4}$	Stefan-Boltzmann constant

TABLE A.2: Density and thermal conductivity of ice (Engineering ToolBox, 2004)

Temperature ($^\circ C$)	**Density** (kg/m^3)	**conductivity** (W/mK)
0	916.2	2.22
-5	917.5	2.25
-10	918.9	2.30
-15	919.4	2.34
-20	919.4	2.39
-25	919.6	2.45
-30	920.0	2.50
-35	920.4	2.57
-40	920.8	2.63
-50	921.6	2.76
-60	922.4	2.90
-70	923.3	3.05
-80	924.1	3.19
-90	924.9	3.34
-100	925.7	3.48

TABLE A.3: Density and heat capacity of air (Engineering ToolBox, 2005)

Temperature (K)	**heat capacity** (kJ/kgK)	**Density** (kg/m^3)
225	1.0027	1.569
250	1.0031	1.412
275	1.0038	1.284
300	1.0049	1.177

TABLE A.4: Density of water (Engineering ToolBox, 2003b)

Temperature ($^\circ C$)	**Density (kg/m^3)**
0.1	999.85
1	999.90
4	999.97
10	999.70
15	999.10
20	998.21
25	997.05

Appendix B

Detailed results

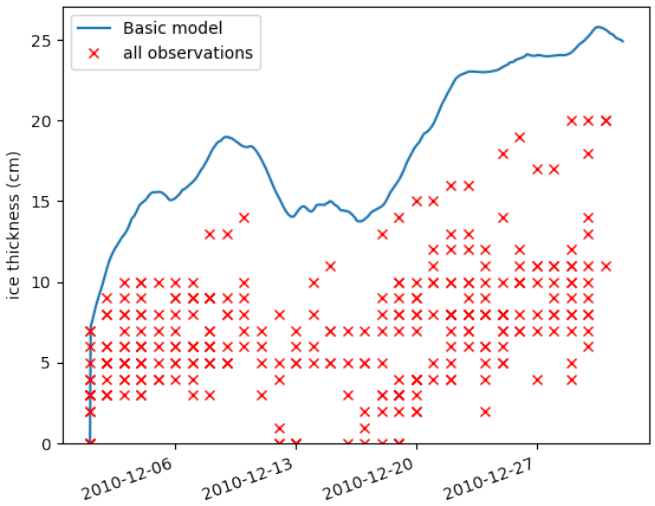

FIGURE B.1: Ice thickness in Friesland 2010 predicted with the the basic model.

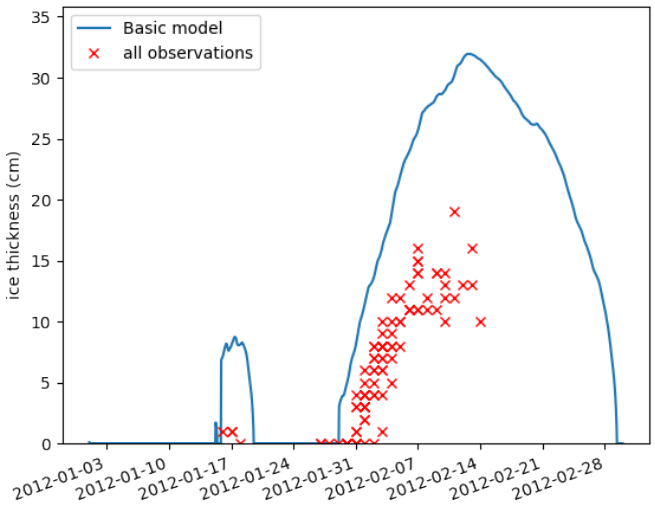

FIGURE B.2: Ice thickness in Friesland 2012 predicted with the the basic model.

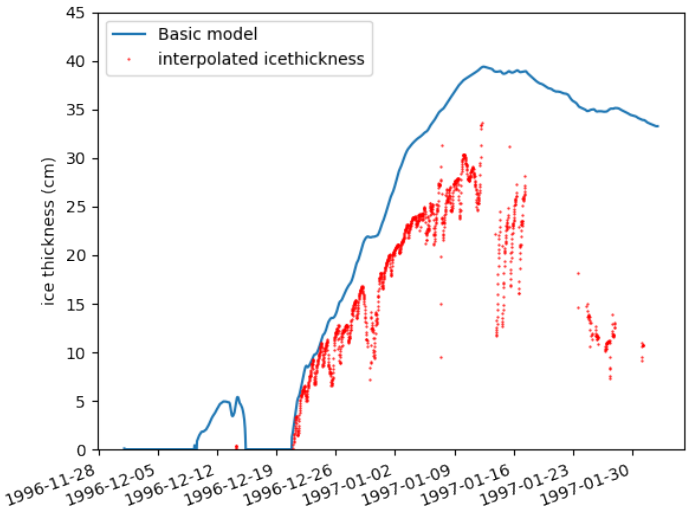

FIGURE B.3: Ice thickness in Cabauw 1996/1997 predicted with the basic model, compared with the interpolated ice thickness data.

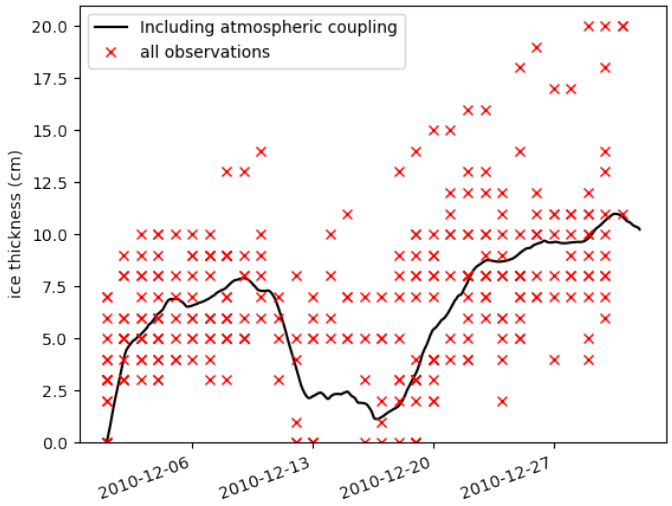

FIGURE B.4: Ice thickness predicted in Friesland 2010 including surface-atmosphere coupling.

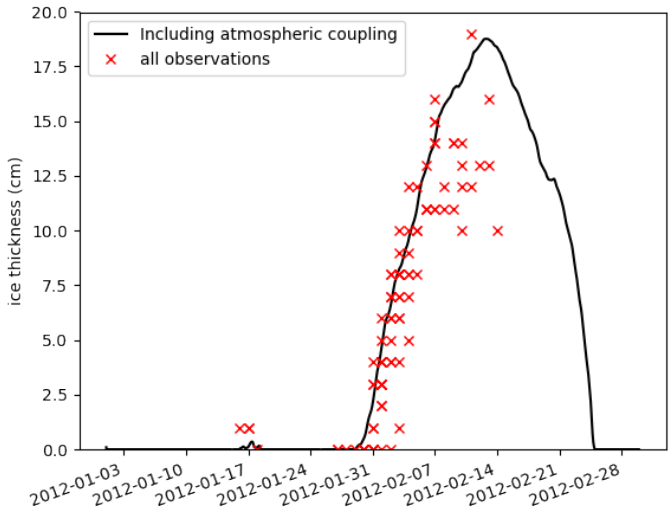

FIGURE B.5: Ice thickness predicted in Friesland 2012 including surface-atmosphere coupling.

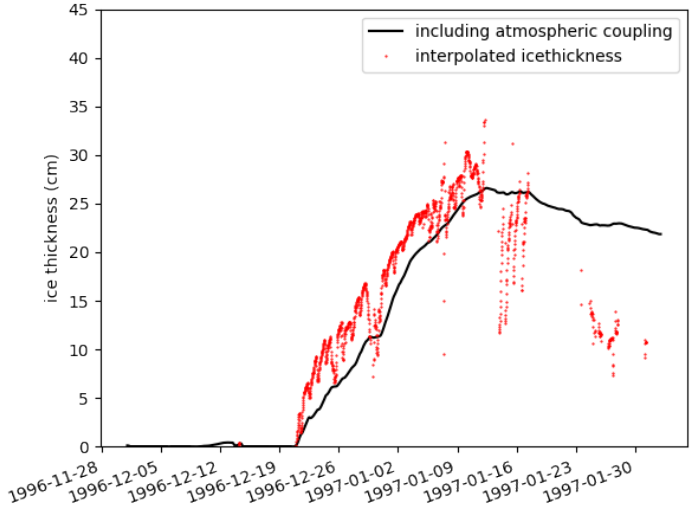

FIGURE B.6: Ice thickness predicted in Cabauw 1996/1997 including surface-atmosphere coupling.

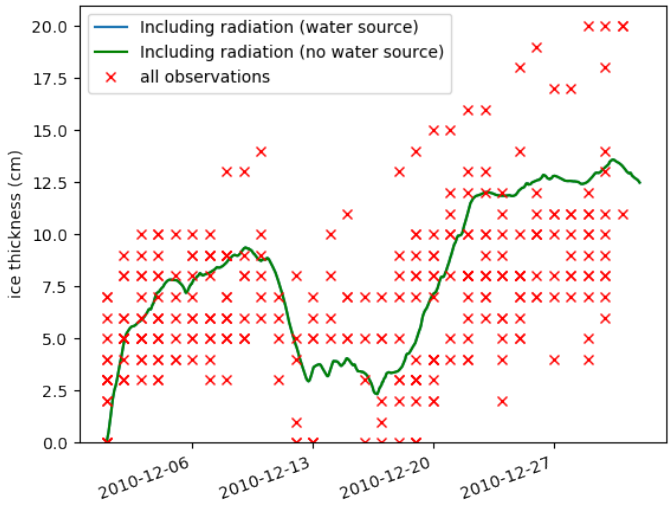

FIGURE B.7: Ice thickness predicted in Friesland 2010 including radiation, cloud coverage, water sources and atmospheric coupling.

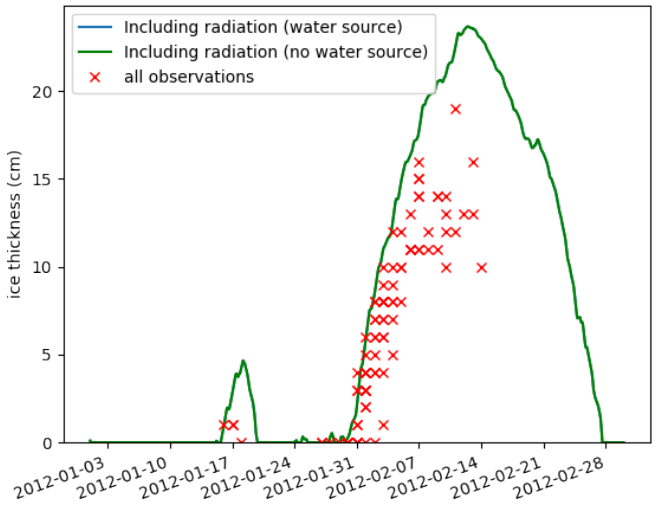

FIGURE B.8: Ice thickness predicted in Friesland 2012 including radiation, cloud coverage, water sources and atmospheric coupling.

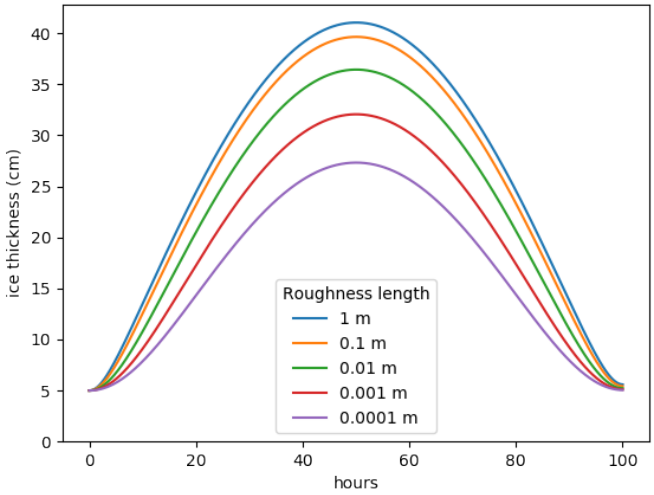

FIGURE B.9: Ice thickness predicted in simulated conditions, with varying roughness lengths.

Bibliography

De Bruijn, E. I. F., Bosveld, F. C., & Van Der Plas, E. V. (2014). An intercomparison study of ice thickness models in the netherlands. *Tellus A: Dynamic Meteorology and Oceanography*, *66*(1). Retrieved from https://www.tandfonline.com/doi/full/10.3402/tellusa.v66.21244

Engineering ToolBox. (2003a). Thermal conductivity of common materials and gases. Retrieved January 2, 2019, from https://www.engineeringtoolbox.com/thermal-conductivity-d_429.html

Engineering ToolBox. (2003b). Water - density, specific weight and thermal expansion coefficient. Retrieved January 1, 2019, from https://www.engineeringtoolbox.com/water-density-specific-weight-d_595.html

Engineering ToolBox. (2004). Ice - thermal properties. Retrieved December 31, 2018, from https://www.engineeringtoolbox.com/ice-thermal-properties-d_576.html

Engineering ToolBox. (2005). Dry air properties. Retrieved January 1, 2019, from https://www.engineeringtoolbox.com/dry-air-properties-d_973.html

Haberman, R. (2014). *Applied partial differential equations with fourier series and boundary value problems* (5th ed.). Pearson.

Howell, J. R., Siegel, R., & Mengüç, M. P. (2010). *Thermal radiation heat transfer* (5th ed.). CRC Press.

Moene, A. & van Dam, J. (2014). *Transfer in the atmosphere- vegetation- soil continuum*. Cambridge university press.